Excitons and biexcitons in symmetric electron-hole bilayers

Ryo Maezono
School of Information Science, JAIST, Asahidai 1-1, Nomi, Ishikawa, 923-1292, Japan

Pablo López Ríos*
Theory of Condensed Matter Group, Cavendish Laboratory, J. J Thomson Avenue, Cambridge CB3 0HE, United Kingdom

Tetsuo Ogawa
Department of Physics, Osaka University, Toyonaka, Osaka 560-0043, Japan

Richard J. Needs
Theory of Condensed Matter Group, Cavendish Laboratory, J. J Thomson Avenue, Cambridge CB3 0HE, United Kingdom
(Received 28 January 2013; published 23 May 2013)

Symmetric electron-hole bilayer systems have been studied at zero temperature using the diffusion quantum Monte Carlo method. A flexible trial wave function is used that can describe fluid, excitonic, and biexcitonic phases. We calculate condensate fractions and pair correlation functions for a large number of densities r_s and layer separations d. At small d we find a one-component fluid phase, an excitonic fluid phase, and a biexcitonic fluid phase, and the transitions among them appear to be continuous. At $d = 0$, excitons appear to survive down to about $r_s = 0.5$ a.u., and biexcitons form at $r_s > 2.5$ a.u.

DOI: 10.1103/PhysRevLett.110.216407 PACS numbers: 71.35.−y, 02.70.Ss, 71.10.−w

Electron-hole bilayer systems in which electrons and holes are generated via doping and confined to separate layers by the application of an electric field have been developed in, for example, GaAs/AlGaAs heterostructures [1]. Other systems have been investigated, such as electron-hole bilayers with very small electron-hole separations at oxide interfaces [2,3] and bilayer graphene systems with approximately equal electron and hole masses [4]. These systems are expected to exhibit rich phase diagrams with Fermi fluid, excitonic superfluid, biexcitonic, and charge density wave phases [5–7]. We have studied the simplest possible such model system, with equal electron and hole populations and equal masses, and parallel infinitely thin two-dimensional layers of variable separation and carrier density. It is important to establish the behavior of this simple system before more complicated cases such as those of unequal electron and hole masses [8] and/or unequal electron and hole densities [9] can be tackled with confidence. Further work will be required to study more realistic systems with anisotropic masses, finite well widths and depths, interface roughness, etc. Theoretical studies of correlation effects in electron-hole bilayers have used methods such as dielectric formulations [10–12], Bardeen-Cooper-Schrieffer theory [8], and diffusion [5,6] and path integral [7] quantum Monte Carlo methods.

We consider paramagnetic, symmetric, electron-hole bilayers consisting of N up- and down-spin electrons and holes of equal masses, $m_e = m_h$, where the distance between the two parallel layers is d. Hartree atomic units are used throughout ($\hbar = |e| = m_e = 4\pi\epsilon_0 = 1$). The Hamiltonian of the infinite system is

$$\hat{H} = -\frac{1}{2}\left(\sum_i \nabla^2_{\mathbf{e}_i} + \sum_i \nabla^2_{\mathbf{h}_i}\right) + \sum_{i<j}\frac{1}{|\mathbf{e}_i - \mathbf{e}_j|} + \sum_{i<j}\frac{1}{|\mathbf{h}_i - \mathbf{h}_j|} - \sum_{i,j}\frac{1}{\sqrt{d^2 + |\mathbf{e}_i - \mathbf{h}_j|^2}}, \quad (1)$$

where $\mathbf{e}_i$ and $\mathbf{h}_j$ are the in-plane position vectors of the ith electron and the jth hole. We use finite simulation cells subject to periodic boundary conditions, and the Coulomb sums are evaluated using two-dimensional Ewald sums [13].

Our results have been obtained with $N = 29$ particles of each type, giving a total of 116 particles, although we have also simulated the system with $N = 57$, corresponding to 228 particles, to investigate finite size effects, which we find to be small. The parameters that define the system are d and the in-layer density parameter $r_s = a/\sqrt{2\pi N}$, where a is the side of the square simulation cell. The d parameter controls the interaction between layers, while r_s controls the interaction within the layers. In this Letter we focus on the density range $r_s < 10$ a.u., and we have not considered the very low density regime within which Wigner crystallization is favorable [5,6]. At large d the electron and hole layers become decoupled and the results for each layer tend towards those for the two-dimensional electron gas [14–16], and when interlayer and intralayer interactions become comparable, i.e., at $d \lesssim r_s$, a paired phase is expected. It has been shown that biexciton formation is energetically favorable at low densities when $d < 0.38$ a.u. [17,18]. Biexciton formation is expected to be suppressed at high densities, and this has been estimated to occur for $r_s \lesssim 10$ a.u. [19].

We have used the variational and diffusion quantum Monte Carlo (VMC and DMC) methods as implemented in the CASINO code [20]. Expectation values are obtained with the VMC method by importance sampled Monte Carlo integration using an importance distribution $|\Psi_T|^2$, where Ψ_T is a suitable trial wave function. Ψ_T contains a number of optimizable parameters whose values are fixed by optimization at each d and r_s. The DMC method is a projector method in which expectation values are computed by approximate solution of the imaginary-time-dependent Schrödinger equation [21,22]. We use the standard "fixed-node" approximation to maintain the fermionic symmetry of the system [23,24]. DMC expectation values are typically more accurate than those from VMC calculations, and in particular the accuracy of DMC energies only depends on the quality of the nodal surface of Ψ_T. We use the standard mixed estimator to evaluate the DMC expectation values reported in this work [22].

In the DMC study of electron-hole bilayers by De Palo *et al.* [5,6], each phase of the system was described by a different wave function, and the relative stability of the phases was determined using the total energy. In our study we use a single flexible wave function form which is capable of describing the Fermi liquid, excitonic superfluid, and biexcitonic phases, and the character of the system at each r_s and d is investigated by computing the expectation values of the electron-hole condensate fraction and the pair-correlation functions (PCFs).

We have used a Slater-Jastrow (SJ) trial wave function,

$$\Psi_T = \exp[J(\mathbf{R})]\det[\phi(\mathbf{e}_i^{\uparrow} - \mathbf{h}_j^{\downarrow})]\det[\phi(\mathbf{e}_i^{\downarrow} - \mathbf{h}_j^{\uparrow})], \quad (2)$$

where $\exp[J(\mathbf{R})]$ is a Jastrow correlation factor that depends on all of the particle positions $\mathbf{R}$, and the pairing orbitals are

$$\phi(\mathbf{r}) = \sum_{l=1}^{n_p} p_l \cos(\mathbf{k}_l \cdot \mathbf{r}) + f(r;L)\sum_{m=0}^{n_c} c_m r^m, \quad (3)$$

where n_p is the plane-wave expansion order, $\mathbf{k}_l$ is the lth shortest reciprocal-space vector, n_c is the polynomial expansion order, $f(r;L)$ is a cutoff function given by $f(r;L) = (1 - r/L)^3\Theta(r - L)$, Θ is the Heaviside step function, and $\{p_l\}$, $\{c_m\}$, and L are optimizable parameters. We constrain $p_l = p_{l'}$ whenever $|\mathbf{k}_l|$ and $|\mathbf{k}_{l'}|$ are in the same star. This form describes a pure fluid phase when $n_p = N$, $p_l \neq 0$ for all l, and $c_m = 0$ for all m, and an excitonic phase when $p_l = 0$ for all l. This wave function cannot describe biexcitons since it only binds antiparallel-spin electron-hole pairs, and biexciton correlations are introduced by the Jastrow factor.

We have used a Drummond-Towler-Needs Jastrow factor [25] consisting of a two-body polynomial u term, to which the electron-electron, hole-hole, and electron-hole Kato cusp conditions are applied [26]. The electron-hole cusp condition is only applicable when $d = 0$, which makes it difficult to obtain results of the same degree of accuracy for $d = 0$ and $d > 0$. To solve this problem we have introduced a "quasicusp" Jastrow factor term, Q, which smoothly introduces the electron-hole cusp condition as $d \to 0$, but we do not use it when $d = 0$ since the u term enforces the exact cusp [27]. The Q term contains a single optimizable cutoff length.

We have used expansion orders of $n_p = 81$ (14 stars of k vectors) and $n_c = 8$. Our wave function contains a total of 47 optimizable parameters at $d = 0$, and 48 at $d > 0$. We have optimized these parameters within VMC calculations using linear least-squares energy minimization [28,29].

The translational-rotational average of the two-body density matrix for electron-hole pairs is

$$\rho_{eh}^{(2)}(r) = \frac{N^2\int|\Psi(\mathbf{R})|^2\frac{\Psi(\mathbf{e}_1+\mathbf{r}',\mathbf{h}_1+\mathbf{r}')}{\Psi(\mathbf{e}_1,\mathbf{h}_1)}\delta(|\mathbf{r}'| - r)d\mathbf{R}\,d\mathbf{r}'}{\Omega^2 2\pi r\int|\Psi(\mathbf{R})|^2 d\mathbf{R}}, \quad (4)$$

where Ω is the area of the simulation cell. The condensate fraction c is defined as the large-r limit of $\rho_{eh}^{(2)}(r)$ normalized so that $c = 1$ when all electrons and holes are bound into excitons [30]. We have evaluated c using the improved estimator of Ref. [31], which we call $c(r)$, see Fig. 1. The condensate fraction is zero for pure one-component and biexcitonic fluid phases.

We also compute the translational-rotational average of the PCF,

$$g_{\alpha\beta}(r) = \frac{\Omega\int|\Psi(\mathbf{R})|^2\delta(\mathbf{r}_\alpha - \mathbf{r}_\beta - \mathbf{r}')\delta(|\mathbf{r}'| - r)d\mathbf{R}\,d\mathbf{r}'}{2\pi r\int|\Psi(\mathbf{R})|^2 d\mathbf{R}}, \quad (5)$$

where α and β are indices that distinguish the four particle types in the system (up- and down-spin electrons and holes). The PCFs allow us to detect biexciton formation,

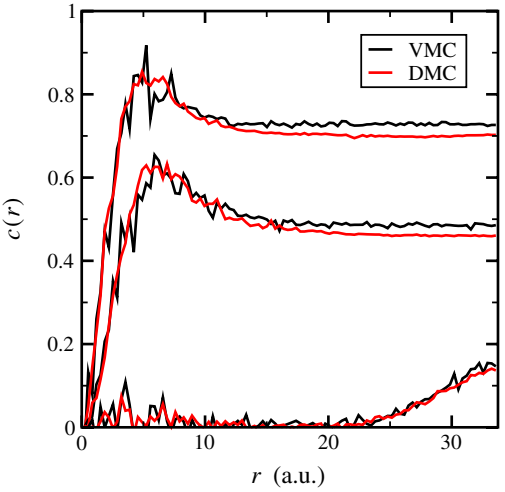

FIG. 1 (color online). VMC and DMC expectation values of $c(r)$ for $r_s = 5$ a.u. and (from top to bottom) $d = 0.3$, 1, and 4 a.u. The systems with $d = 0.3$ and 1 a.u. are in the excitonic phase, and that with $d = 4$ a.u. is in the fluid phase.

distinguishing the biexcitonic phase from the one-component fluid, for both of which $c = 0$.

We used a target walker population of 1280 configurations and a time step of 0.01 a.u. for the DMC calculations. We verified that the energy, condensate fraction, and PCF do not change significantly when the time step was reduced from this value. The accuracy of a trial wave function can be measured by the differences between expectation values calculated with the VMC and DMC methods. We find that these differences are small. To investigate the convergence of our results with respect to the quality of the wave function, we have also performed calculations using the more sophisticated Slater-Jastrow-backflow wave functions for selected cases. These wave functions incorporate a backflow transformation in which the particle coordinates are replaced by "quasiparticle" coordinates [32,33], which adds 27 optimizable parameters to the wave function. The introduction of backflow results in significant changes in the computed expectation values at small values of d but, as d increases, the difference declines. This indicates that the description of in-layer correlations afforded by the SJ wave function is very good, while the description of correlations between the motion in the electron and hole layers is not as good.

We have computed $c(r)$ within VMC and DMC calculations, and have evaluated the condensate fractions as the average of $c(r)$ over the region of the plateau at large r [27]. Three examples of $c(r)$ functions are shown in Fig. 1. The VMC and DMC values of the condensate fraction differ by less than 3% in each case. In the fluid phase $c(r)$ is close to zero for small values of r, but it rises in value as r reaches the edge of the simulation cell. We interpret this as an effect due to the finite size of the simulation cell, and take c to be zero when this feature is present.

Our results for the condensate fraction agree with those of Ref. [5] for large d, but we tend to obtain larger condensate fractions for small d. Our main results for the condensate fractions are shown in Figs. 2 and 3. Figure 2(a) shows that for small values of d and $r_s \geq 3$ a.u. the condensate fraction curves fall to zero with increasing r_s, which can be attributed to the formation of biexcitons. Biexciton formation is favorable only at small d, because at large d the in-plane repulsion between like charges dominates the weak e-h attraction. Figure 3 shows the condensate fraction as a function of r_s and d, including smoothed phase boundaries and other contour lines, and a line that locates the maximum c for each r_s. Since biexciton formation is the only likely mechanism by which c can be reduced as d decreases, this line delimits the region where biexciton formation takes place. The maximum condensate fraction for large values of r_s occurs at $d = 0.4$ a.u., and c increases with r_s reaching, for instance, $c = 0.95$ at $r_s = 15$ a.u.

Studies of the bilayer system with two anti-parallel-spin electrons and holes have shown that biexciton formation is

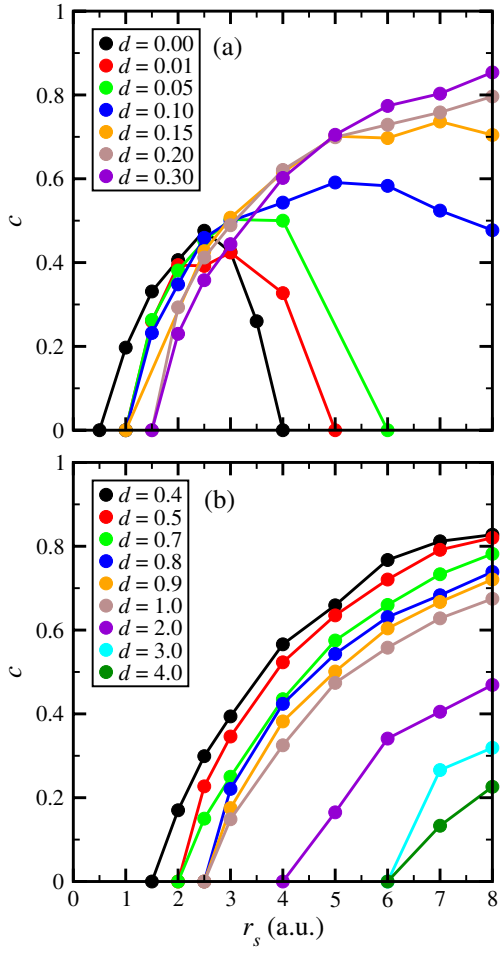

FIG. 2 (color online). DMC condensate fraction as a function of r_s at (a) $d < 0.4$ a.u. and (b) $d \geq 0.4$ a.u.

energetically favorable for $d < 0.38$ a.u. [17,18]. We have found that biexciton formation is favorable in extended systems at large r_s for values of d similar to those for the isolated biexciton [17,18], but that biexcitons do not form below $r_s \simeq 2.5$ a.u., see Fig. 2.

Condensate fractions calculated using a bosonic dipole model have been reported in the literature [34–36]. The behavior of this bosonic system with a repulsive interaction differs qualitatively from that of the electron-hole bilayer model at small d, since the repulsive interaction is not capable of describing biexciton formation. At large d there is a quantitative difference between the models since the repulsive dipole-dipole interaction differs from the in-layer Coulomb interaction. We find that the bosonic dipole model gives condensate fractions which are in good quantitative agreement with our results within the excitonic phase for $r_s = 7$–8 a.u. and $d > 0.4$ a.u.

The PCFs within the e-h bilayer at $r_s = 4$ a.u. for $d = 0$, 0.4, and 3 a.u. are shown in Fig. 4 [27]. For $d = 3$ a.u. the coupling between the layers is weak and the system is in the fluid state. The Fermi hole for same-spin e-e/h-h pairs is wider than the correlation hole for

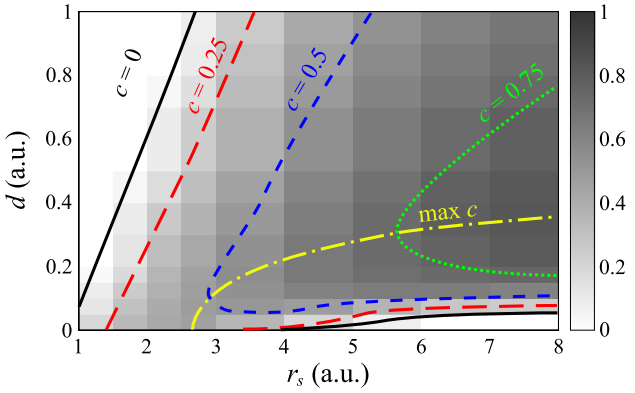

FIG. 3 (color online). The estimated DMC condensate fraction as a function of r_s and d. Phase boundaries are represented by solid lines, and contours of the condensate fraction are shown as long-dashed, short-dashed, and dotted lines. The dot-dashed line indicates the location of the maximum c for each r_s, below which some degree of biexciton formation takes place.

opposite-spin e-e/h-h pairs. The PCFs for same and opposite spin e-e/h-h correlations in Fig. 4(a) are indistinguishable from those calculated for the two-dimensional electron gas ($d \to \infty$) [27]. The enhancement of the same and opposite spin e-h PCFs at small r is very weak because of the large layer separation.

The PCF for antiparallel-spin e-h pairs at $d = 0.4$ a.u., see Fig. 4(b), is strongly peaked at zero in-plane separation, while the parallel-spin e-h PCF shows a shallow trough with a PCF of 0.97 at about $r = 3$ a.u. and a small peak at $r = 0$ a.u. The difference between these two PCFs is due to the fact that our wave function explicitly binds antiparallel-spin electron-hole pairs. The PCF for parallel-spin e-e/h-h pairs is strongly suppressed at small separations, and is nearly identical to the parallel-spin e-h/h-h PCF at $d = 4$ a.u. The PCF for antiparallel-spin e-e/h-h pairs shows a small peak with a PCF of 1.15 at $r \simeq 2.4$ a.u., significantly closer to the origin than the peak in the corresponding PCF at $d = 4$ a.u. There is almost no correlation hole in this PCF, reflecting the fact that opposite-spin excitons are allowed to be close to each other. The PCF is very close to unity for $r > 10$ a.u. The PCFs demonstrate the existence of an excitonic phase at $d = 0.4$ a.u.

The PCFs for $r_s = 4$ a.u. and $d = 0$ in the biexcitonic phase, depicted in Fig. 4(c), show very different features. The PCFs show substantial long range oscillations which are not present in the excitonic or one-component fluid phases. The PCFs are strongly peaked at the origin for both parallel- and antiparallel-spin e-h pairs, while the PCF for antiparallel-spin e-e/h-h pairs shows a fairly strong peak and the PCF for parallel-spin e-e/h-h pairs is close to zero for $r < 0.4$ a.u. Clearly the particles are aggregating into an object larger than an exciton as the PCF for antiparallel-spin e-e/h-h pairs is substantial at small r. The fact that the parallel spin e-e/h-h PCF is essentially zero at small r tells us that the object in question contains, at most, one particle of each type. Direct integration of the PCFs confirms that the object contains one particle of each of the four types, and that it is therefore a biexciton. The formation of objects larger than a biexciton is impeded by Pauli exclusion. Noting also the oscillations in the $d = 0$ PCFs which decay with distance, we can identify this phase as a biexcitonic fluid. The diameter of the biexciton, measured as the median distance between the anti-parallel-spin electrons, is about 1.46 a.u. At $r_s = 6$ and $d = 0$ we estimate the biexciton diameter to be 1.48 a.u. [27].

In summary, we use a wave function form of sufficient flexibility to describe the fluid, excitonic, and biexcitonic phases. As the excitonic phase lies between the fluid and biexcitonic phases, we identify the phase transitions by the existence of a nonzero excitonic condensate fraction, and

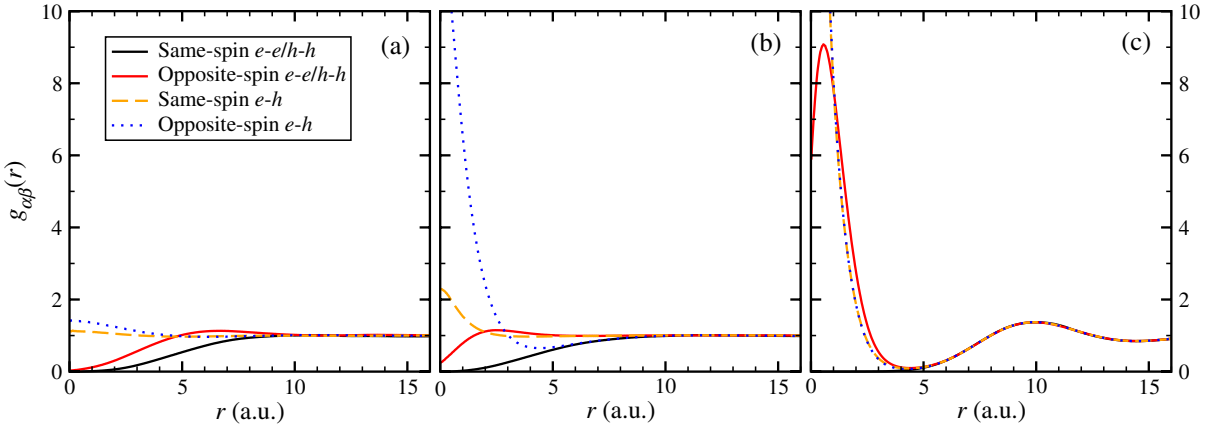

FIG. 4 (color online). DMC PCFs as a function of the interparticle distance r at a density of $r_s = 4$ a.u. and interlayer separations of (a) $d = 3$ a.u. in the fluid phase, (b) $d = 0.4$ a.u. in the excitonic phase, and (c) $d = 0$ a.u. in the biexcitonic phase. Note the strong enhancement of the opposite-spin e-h PCF at small r in the excitonic phase, and the strong enhancement of both the opposite-spin and same spin e-h PCFs at small r in the biexcitonic phase.

the fluid and biexcitonic phases can be distinguished by their characteristic PCFs. The good agreement of our VMC and DMC expectation values suggests that our results are of good quality, as does the agreement between the results obtained using the SJ and Slater-Jastrow-backflow wave functions. Excitons are unstable to biexciton formation at low densities and $d < 0.38$ a.u. in the bilayer system considered here [17,18]. For small values of d, we have found that biexcitons can survive down to about $r_s = 2.5$ a.u., which is a considerably higher density than suggested previously [19].

R. M. is grateful for financial support from KAKENHI Grants No. 23104714 and No. 22104011, and from the Tokuyama Science Foundation. P. L. R. and R. J. N. acknowledge financial support from the Engineering and Physical Sciences Research Council (EPSRC) of the United Kingdom. T. O. acknowledges support from the JSPS through its FIRST Program, and from DYCE via KAKENHI Grant No. 20104008. The authors wish to thank Ms. Mitsumi Fujita for her assistance with the calculations.

*pl275@cam.ac.uk

[1] K. D. Gupta, A. F. Croxall, J. Waldie, C. A. Nicoll, H. E. Beere, I. Farrer, D. A. Ritchie, and M. Pepper, Adv. Condens. Matter Phys. **2011**, 727958 (2011).
[2] R. Pentcheva, M. Huijben, K. Otte, W. E. Pickett, J. E. Kleibeuker, J. Huijben, H. Boschker, D. Kockmann, W. Siemons, G. Koster, H. J. W. Zandvliet, G. Rijnders, D. H. A. Blank, H. Hilgenkamp, and A. Brinkman, Phys. Rev. Lett. **104**, 166804 (2010).
[3] M. Huijben, D. Kockmann, J. Huijben, J. E. Kleibeuker, A. van Houselt, G. Koster, D. H. A. Blank, H. Hilgenkamp, G. Rijnders, A. Brinkman, and H. J. W. Zandvliet, Phys. Rev. B **86**, 035140 (2012).
[4] A. Perali, D. Neilson, and A. R. Hamilton, Phys. Rev. Lett. **110**, 146803 (2013).
[5] S. De Palo, F. Rapisarda, and G. Senatore, Phys. Rev. Lett. **88**, 206401 (2002).
[6] G. Senatore and S. De Palo, Contrib. Plasma Phys. **43**, 363 (2003).
[7] J. Schleede, A. Filinov, M. Bonitz, and H. Fehske, Contrib. Plasma Phys. **52**, 819 (2012).
[8] A. L. Subasi, P. Pieri, G. Senatore, and B. Tanatar, Phys. Rev. B **81**, 075436 (2010).
[9] M. M. Parish, F. M. Marchetti, and P. B. Littlewood, Europhys. Lett. **95**, 27 007 (2011).
[10] R. K. Moudgil, G. Senatore, and L. K. Saini, Phys. Rev. B **66**, 205316 (2002).
[11] K. S. Singwi, M. P. Tosi, R. H. Land, and A. Sjölander, Phys. Rev. **176**, 589 (1968).
[12] K. I. Golden, G. J. Kalman, P. Hartmann, and Z. Donkó, Contrib. Plasma Phys. **52**, 130 (2012).
[13] D. E. Parry, Surf. Sci. **49**, 433 (1975); **54**, 195(E) (1976).
[14] B. Tanatar and D. M. Ceperley, Phys. Rev. B **39**, 5005 (1989).
[15] C. Attaccalite, S. Moroni, P. Gori-Giorgi, and G. B. Bachelet, Phys. Rev. Lett. **88**, 256601 (2002).
[16] N. D. Drummond and R. J. Needs, Phys. Rev. B **79**, 085414 (2009).
[17] C. Schindler and R. Zimmermann, Phys. Rev. B **78**, 045313 (2008).
[18] R. M. Lee, N. D. Drummond, and R. J. Needs, Phys. Rev. B **79**, 125308 (2009).
[19] P. B. Littlewood and X. Zhu, Phys. Scr. **T68**, 56 (1996).
[20] R. J. Needs, M. D. Towler, N. D. Drummond, and P. L. Ríos, J. Phys. Condens. Matter **22**, 023201 (2010).
[21] D. M. Ceperley and B. J. Alder, Phys. Rev. Lett. **45**, 566 (1980).
[22] W. M. C. Foulkes, L. Mitas, R. J. Needs, and G. Rajagopal, Rev. Mod. Phys. **73**, 33 (2001).
[23] J. B. Anderson, J. Chem. Phys. **63**, 1499 (1975).
[24] J. B. Anderson, J. Chem. Phys. **65**, 4121 (1976).
[25] N. D. Drummond, M. D. Towler, and R. J. Needs, Phys. Rev. B **70**, 235119 (2004).
[26] T. Kato, Comm. Pure Appl. Math. **10**, 151 (1957).
[27] See Supplemental Material at http://link.aps.org/supplemental/10.1103/PhysRevLett.110.216407 for additional results, a full description of the Jastrow factor, an analysis of the convergence of the results, and a visualization of the different phases in real space.
[28] J. Toulouse and C. J. Umrigar, J. Chem. Phys. **126**, 084102 (2007).
[29] C. J. Umrigar, J. Toulouse, C. Filippi, S. Sorella, and R. G. Hennig, Phys. Rev. Lett. **98**, 110201 (2007).
[30] C. N. Yang, Rev. Mod. Phys. **34**, 694 (1962).
[31] G. E. Astrakharchik, J. Boronat, J. Casulleras, and S. Giorgini, Phys. Rev. Lett. **95**, 230405 (2005).
[32] Y. Kwon, D. M. Ceperley, and R. M. Martin, Phys. Rev. B **48**, 12 037 (1993).
[33] P. L. Ríos, A. Ma, N. D. Drummond, M. D. Towler, and R. J. Needs, Phys. Rev. E **74**, 066701 (2006).
[34] G. E. Astrakharchik, J. Boronat, I. L. Kurbakov, and Yu. E. Lozovik, Phys. Rev. Lett. **98**, 060405 (2007).
[35] G. E. Astrakharchik, J. Boronat, J. Casulleras, I. L. Kurbakov, and Yu. E. Lozovik, Phys. Rev. A **75**, 063630 (2007).
[36] A. Filinov and M. Bonitz, Phys. Rev. A **86**, 043628 (2012).